Novel Reactive Compatibilization Strategy on Immiscible Polypropylene and Polystyrene Blend

Chen-Jui Hung, Hung-Yang Chuang, Feng-Chih Chang

Institute of Applied Chemistry, National Chiao-Tung University, Hsin-Chu, Taiwan, 30043

Received 10 May 2006; accepted 17 July 2006
DOI 10.1002/app.25201
Published online 27 September 2007 in Wiley InterScience (www.interscience.wiley.com).

ABSTRACT: Polypropylene (PP) and polystyrene (PS) are immiscible and incompatible. Since both PP and PS components possess no reactive functional group, reactive compatibilization of a PP/PS blend is impossible unless certain reactive functional groups are imparted to either PP or PS. In this study we provide a simple approach to reactively compatibilize the nonreactive PP/PS blend system by physically functionalizing PP and PS with the addition of maleic anhydride grafted PP (PP-*g*-MA) and styrene maleic anhydride random copolymer (SMA), respectively. An epoxy monomer, serving as a coupler and possessing four epoxy groups able to react with the maleic anhydride of PP-*g*-MA and SMA, was then added during melt blending. Observations of the finer PS domain sizes and improved mechanical properties support the plausibility of reactive compatibilization of this nonreactive PP/PS blend by combining physically functionalized PP and PS with tetra-glycidyl ether of diphenyl diamino methane (TGDDM) in a one-step extrusion process. © 2007 Wiley Periodicals, Inc. J Appl Polym Sci 107: 831–839, 2008

Key words: polymer blends; reactive compatibilization; polypropylene; polystyrene

INTRODUCTION

Polymer blends have attracted great attention both industrially and academically because of their flexibility and versatility to create new materials with desired properties from existing polymers. However, it is nearly impossible to obtain a useful polymer blend material without compatibilization because most randomly selected polymer pairs are immiscible and incompatible, with only a few exceptions. As a result, compatibilization of immiscible and incompatible polymer blends has become a critically important topic and research field in the past few decades.[1,2]

Compatibilization of immiscible and incompatible polymer blends can be achieved by using various nonreactive and reactive compatibilizers. Nonreactive graft or block copolymers are successfully employed as efficient compatibilizers because they are able to locate at the interface and act as emulsifiers to lower the interfacial tension.[2–4] Due to their high molecule weight nature, however, large portions of the block copolymers prefer to form micelles in either homopolymer phases, rather than residing along the interfaces. Moreover, only a few block and graft copolymers suitable as compatibilizers are readily available commercially, and most of them require a separate synthesis process and are costly. Those shortcomings make reactive compatibilization an alternative and more practical way to produce useful polymer blends.[5–8] Instead of premade block or graft copolymers, reactive compatibilization forms copolymers *in situ* during the melt blending process if the constituent polymers contain certain functional groups. Since the reaction of functional groups occurs at the interfaces, the *in situ* formed copolymers tend to stay at the interface, providing a better compatibilization effect.

Polypropylene (PP) and polystyrene (PS) represent two of the most common commodity polymers in the world. Polymer blends of PP and PS have always been an interesting topic for resin suppliers and compounders because of the potential to recycle the large-volume waste. PP and PS are immiscible, and much work on compatibilizing PP/PS blends has been done by using SBS, SEBS, SEP, and SIS block copolymers as nonreactive compatiblizers.[9–11] However, relatively few studies on reactive compatibilization of the PP/PS blend have been reported because of a lack of functional groups in both PP and PS. Dicumyl peroxide was employed by Xie and Zheng[12] to generate *in situ* PP PP-*g*-PS graft copolymer in a one-step extrusion process and the dispersed particle size was greatly reduced. Kim et al.[13] found that the molecular architecture and functional group inhomogeneity of *in situ* compatibilizers strongly affects the compatibilizing efficiency, rheology, and morphology. Sun et al.[14] reported that an *in situ* compatibilization of the PP/PS blend was achieved by using Friedel-Crafts benzene ring alkylation

Correspondence to: F.-C. Chang (changfc@mail.nctu.edu.tw).

Journal of Applied Polymer Science, Vol. 107, 831–839 (2008)

TABLE I
Properties of Materials Used in This Study

	MA (wt%)	Tg (°C)	Tm (°C)	Tc (°C)	Melt index (g/10min)
PP	0	—	165.6	113.1	7.9
PS	0	92.9	—	—	8.7
PP-g-MA	0.8	—	160.9	127.9	17.3
SMA	8	118.7	—	—	5.3

of PS through reactive extrusion, which resulted in improved tensile elongation.

It is known that maleic anhydride grafted (PP-*g*-MA)[15–17] and styrene maleic anhydride (SMA)[6] with low MA content are miscible with PP and PS, respectively. In this study we attempted to physically functionalize both PP and PS by adding a small quantity of commercially available PP-*g*-MA and SMA, respectively. By doing so, the reactive compatibilization of the nonreactive blend becomes possible. A multifunctional epoxy, proven to be an effective coupler in reactive compatibilization,[7,8] is then introduced into the blend and is capable of reacting with the maleic anhydride of SMA and PP-*g*-MA simultaneously at the interface to form various PS-*co*-epoxy-*co*-PP copolymers during the melt-blending process. The chemistry, morphology, and mechanical properties of the compatibilized PP/PS blend will be systematically revealed and discussed.

EXPERIMENTAL

Materials

Homopoymer PP, a general-purpose grade PC-366-5, was obtained from Taiwan Polypropylene. PS, PG-33, was purchased from Chi Mei (Taiwan). PP-*g*-MA with an MA content 0.8 wt% was supplied by UniRoyal Chemical (Geismar, LA). SMA copolymer containing 8 wt% maleic anhydride, Dylark 232, was purchased from ARCO Chemical (Newton Square, PA). The epoxy resin, tetra-glycidyl ether of diphenyl diamino methane (TGDDM), trademark NPEH-434, was purchased from the Nan Yea Plastics (Taiwan). Tables I and II list the

TABLE II
Chemical Structure of Materials Used in This Study

PP

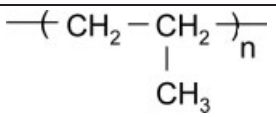

PS

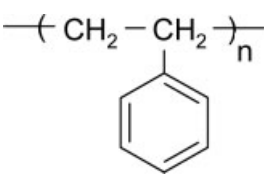

SMA

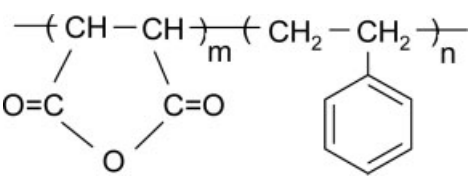

PP-g-MA

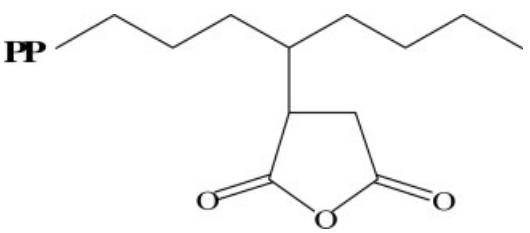

TGDDM

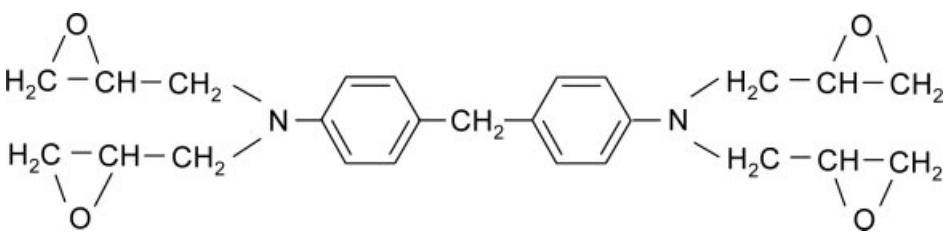

TABLE III
Processing Conditions of Extrusion and Injection Molding

	Temperature (°C)											
Stage	1	2	3	4	5	6	7	8	9	Die	Nozzle	Mold
Extrusion	150	180	190	200	220	230	230	240	240	245	—	—
Injection	225	230	235	—	—	—	—	—	—	—	240	70

properties and the chemical structures of the materials used in this work, respectively.

Extrusion and injection molding

All blends were dry-mixed first and the melt-blending process was carried out with a 30-mm corotating intermeshing twin-screw extruder (L/D = 36, Sino Alloy Machinery, Taiwan) with a rotational speed of 180 rpm. The standard ASTM test specimens were prepared by an Arburg 3 oz. injection-molding machine. Prior to melt blending and injection molding, all pellets were dried in an oven at 80°C for 4 h. The detailed processing conditions for extrusion and injection molding are summarized in Table III.

Infrared spectroscopy

All infrared spectra were obtained at a resolution of 1 cm^{-1} on a Nicolet AVATAR 320 FTIR Spectrometer at 25°C.

Torque versus time measurement

To verify potential chemical reaction among PP-*g*-MA, SMA, and TGDDM based on the viscosity increase (torque vs. time), 45 g of the selected composition was tested at 200°C and 40 rpm in a Brabender Plasti-Corder, type PLD 651.

Thermal properties

Thermal properties of pure components and blends were investigated on a TA instrument DSC 2010 with a sample weight of 5–10 mg. All samples were heated to 220°C and subsequently annealed for 3 min, then cooled to 80°C to determine the crystallization temperature (Tc) of the polypropylene. After the cooling process, the sample was reheated to 220°C to determine the melting temperature (Tm) of the polypropylene. Both heating and cooling rates were 10°C/min.

Scanning electron microscopy

The morphologies were examined by a scanning electron microscope (SEM) at accelerating voltage 20 kV (Model S-570, Hitachi, Japan) from cryogenically fractured specimens in the plane perpendicular to the flow direction of injection molding. Samples were etched with tetrahydrofuran (THF) to dissolve the PS phase out of the blends. The fractured surfaces of specimens were coated with a thin film of gold to prevent charging.

Mechanical properties

An Instron Universal Testing Machine (Canton, MA, Model 4201) was used to measure the mechanical properties of the incompatibilized and compatibilized blends. Tensile tests were measured according to the ASTM D638 method with a crosshead speed of 5 mm/min used at ambient conditions. Flexural tests were measured according to the ASTM D790 method with 50 mm span and 5 mm/min test speed at ambient conditions.

RESULTS AND DISCUSSION

Chemistry

In reactive compatibilization, the chemical reactions between the functional groups of the reactive copolymers and the coupler are expected to occur and to form various desired *in situ* formed compatibilizers during the melt-blending process. The formation of

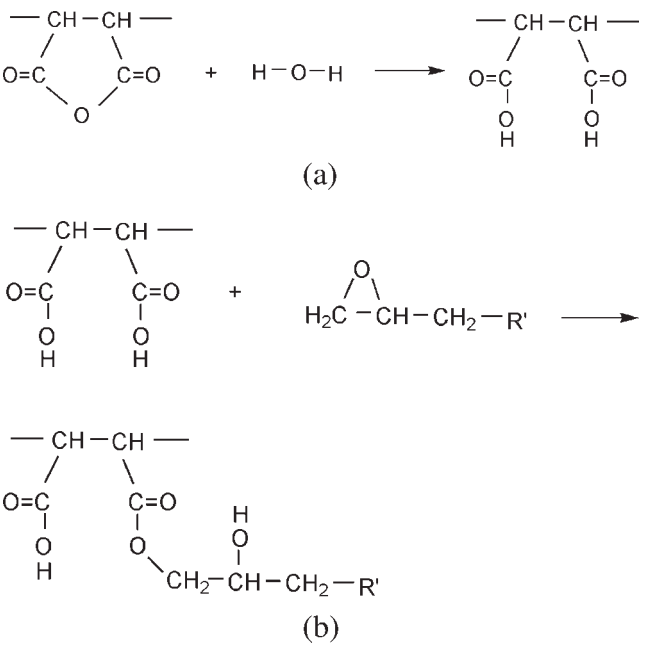

Scheme 1 The simplified reaction mechanism between anhydride and epoxy. (a) Ring-opening reaction of anhydride by water vapor. (b) Reaction of ring-opened anhydride with epoxy.

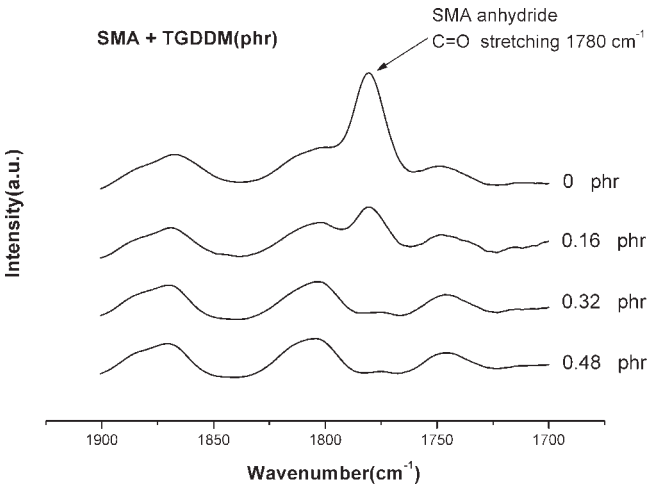

Figure 1 FTIR spectrum for SMA melt-blended with various amounts of TGDDM in the 1900–1700 cm^{-1} region.

the *in situ* compatibilizers is critically dependent on the relative reactivities between functional groups of the reactive polymers with the coupler, processing temperature, time, and mixing efficiency. The main reaction involved in this study is the reaction of the anhydride groups of SMA and PP-*g*-MA with the epoxy groups of the TGDDM. As illustrated in Scheme 1(a), the reaction can be initiated by atmospheric water vapor or the residual moisture content in the feeding materials, proceeding in the ring-opening reaction. The ring opened anhydride group will then react with the epoxy group of TGDDM as shown in Scheme 1(b). The reaction will basically take place along the interfaces; thus, the *in situ* formed PP-*g*-MA-*co*-TGDDM-*co*-SMA copolymers tend to stay at the interface as interfacial emulsifiers. As a result, the compatibilization is more efficient than a nonreactive block or graft copolymer.

FTIR spectroscopy

Fourier transform infrared (FTIR) spectroscopy is a powerful tool for observing the reactions between the functional groups of anhydride of SMA and PP-*g*-MA and the epoxy group of TGDDM. Figure 1 shows the superimposed FTIR spectra of mixtures of SMA containing various amounts of TGDDM after melt blending. The peak in the 1780 cm^{-1} is assigned to carbonyl stretching mode of the maleic anhydride group of SMA. The intensity of the characteristic peak of the maleic anhydride decreases with increasing the quantity of the TGDDM, due to the reaction between TGDDM and SMA, as expected. With the addition of 0.32 phr TGDDM, the peak at 1780 cm^{-1} nearly disappeared, implying that nearly all MA groups are consumed during the melt-blending process. The FTIR spectrum of the SMA containing 0.48 phr TGDDM shows that the peak at 1780 cm^{-1} is totally missed, an indication of total consumption of the MA groups.

The FTIR spectra of PP-*g*-MA, TGDDM, and a melt-blended mixture of PP-*g*-MA with 3 phr TGDDM are shown in Figure 2. The characteristic peak at 1770 cm^{-1} of the anhydride group from the PP-g MA decreases significantly in the presence of TGDDM, compared to that of the pure PP-*g*-MA. The intensity decrease of the characteristic peak can be attributed to the partial reaction of TGDDM and PP-*g*-MA during the melt-blending process. Based on the FTIR findings, it is expected that TGDDM will react simultaneously with SMA and PP-*g*-MA during melt-blending and form various PP-*g*-MA-*co*-TGDDM-*co*-SMA copolymers along the interfaces to serve as the compatibilizers of the immiscible PP/PS blend.

Torque versus time

Torque measurement was utilized to obtain qualitative information on the chemical reactivity in this study. Figure 3 plots the torque versus time curves

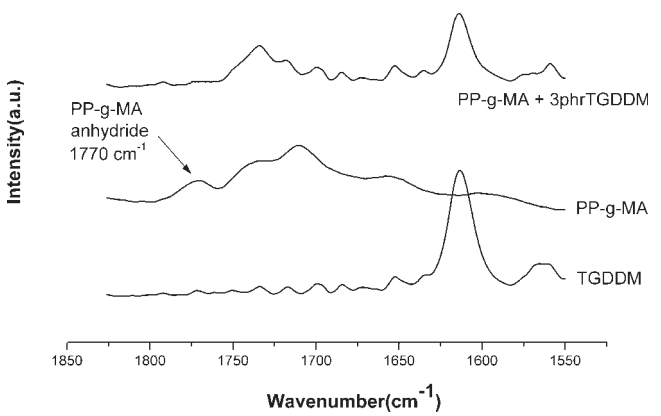

Figure 2 FTIR spectrum for PP-*g*-MA melt-blended with 3 phr TGDDM in the 1900–1700 cm^{-1} region.

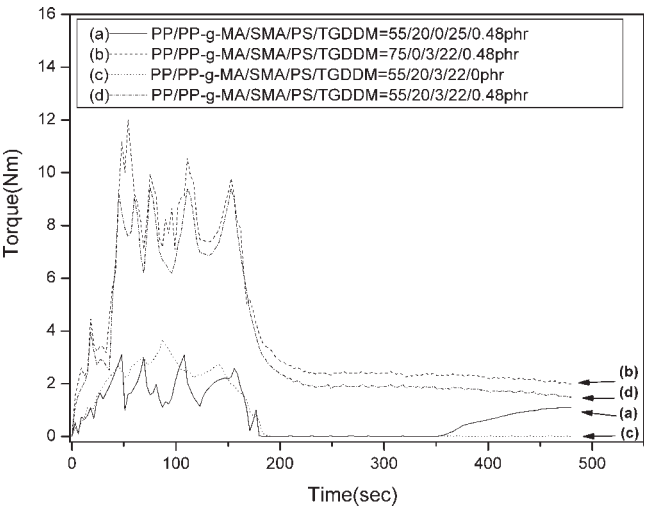

Figure 3 Plot of torque versus time for various PP-*g*-MA/SMA/TGDDM blends. Blends were prepared at 240°C and 40 rpm in a Brabender mixer.

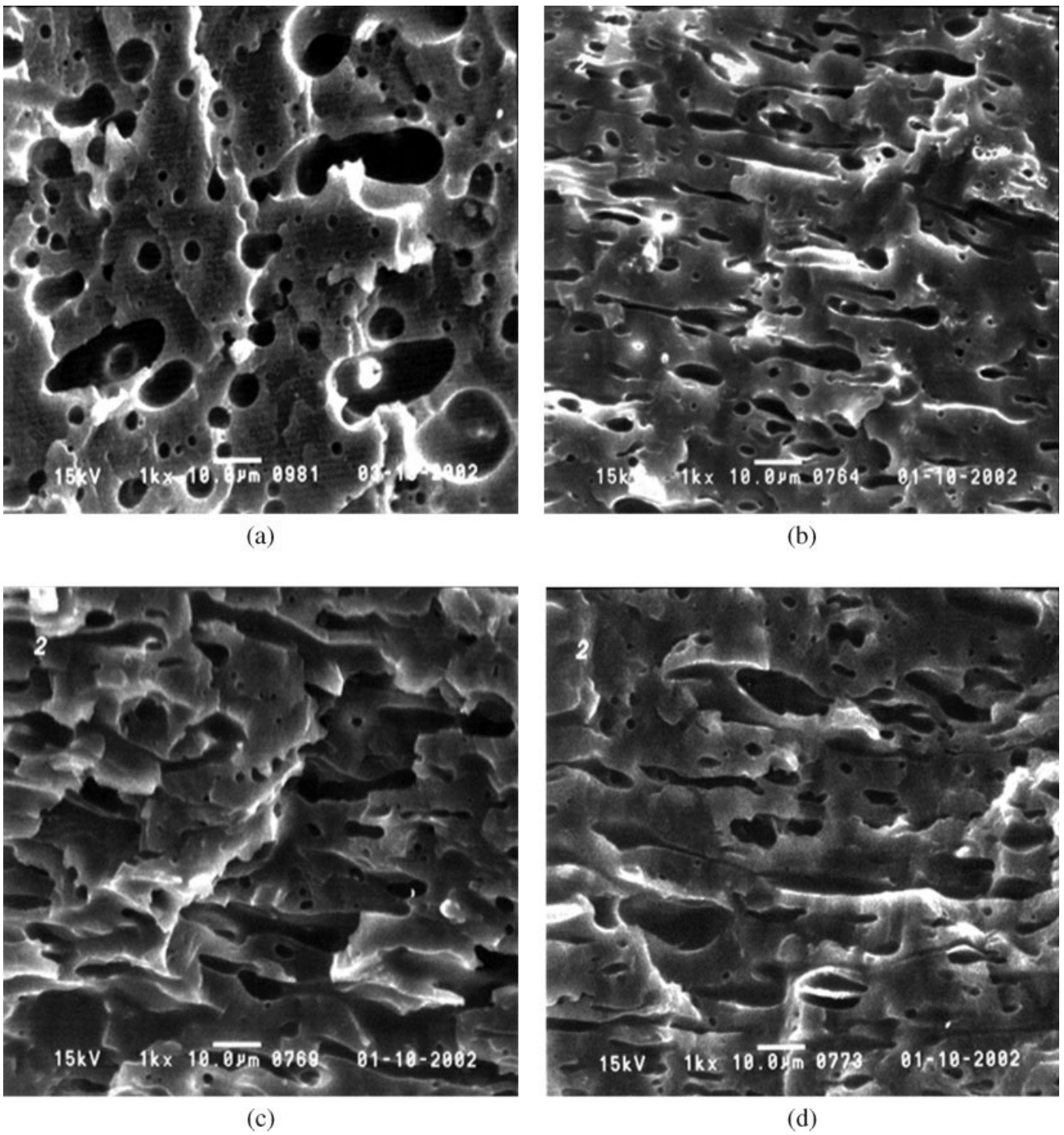

Figure 4 SEM micrographs of cryogenic fractured surfaces for PP/PS and various physically functionalized PP/PS blends (×1000): (a) PP/PS = 75/25; (b) PP/PP-*g*-MA/SMA/PS = 55/20/1/24; (c) PP/PP-*g*-MA/SMA/PS = 55/20/2/23; (d) PP/PP-*g*-MA/SMA/PS = 55/20/3/22.

for various PP-*g*-MA/SMA/TGDDM blends at the processing conditions of chamber temperature 200°C at rotational speed 40 rpm. PP-*g*-MA and SMA pellets were dry-blended and fed into the mixer. TGDDM was then added at time t = 180 s, where the torque value reached was steady and ensured at the melt state. The torque value of PP/PP-*g*-MA/SMA/PS/TGDDM = 55/20/3/22/0.48 phr [Fig. 3(a)] and PP/PP-*g*-MA/SMA/PS/TGDDM = 75/0/3/22/0.48 phr [Fig. 3(b)] suddenly dropped to nearly zero with the addition of TGDDM because of the low molecule weight nature of TGDDM, functioning as a lubricant before reacting with maleic anhydride. After a certain reaction time the torque value of PP/PP-*g*-MA/

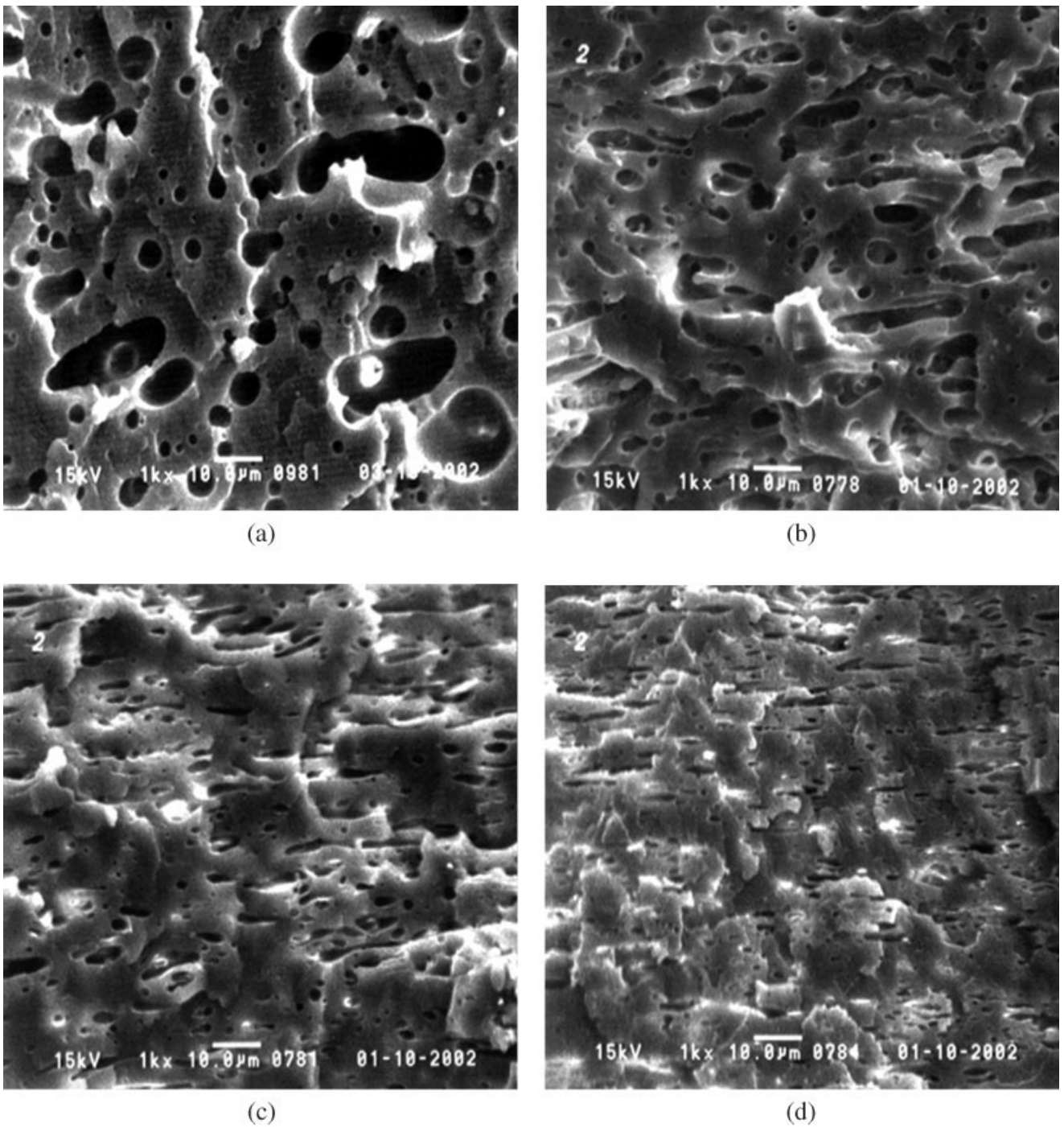

Figure 5 SEM micrographs of PP/PP-*g*-MA/SMA/PS = 70/20/1/24 blends containing (a) PP/PS-75/25; (b) 0.16 phr; (c) 0.32 phr; (d) 0.48 phr of TGDDM.

SMA/PS/TGDDM = 55/20/3/22/0.48 phr [Fig. 3(a)] increases only slightly while the torque of PP/PP-*g*-MA/SMA/PS/TGDDM = 75/0/3/22/0.48 phr [Fig. 3(b)] rises sharply. This indicates that the reaction rate of SMA and TGDDM is significantly faster than that of PP-*g*-MA and TGDDM during melt-blending. The sharper increased torque value also implies that the degree of molecular weight increase of SMA is higher than that of PP-*g*-MA with the addition of the multifunctional TGDDM. The torque value of PP/PP-*g*-MA/SMA/PS/TGDDM = 55/20/3/22/0 phr [Fig. 3(c)] is close to zero, implying no reaction or interaction between PP-*g*-MA and SMA. However, the torque value of PP/PP-*g*-MA/SMA/PS/TGDDM = 55/20/

TABLE IV
DSC Results of Pure Component and Corresponding Blends

PP/PP-g-MA/SMA/PS/TGDDM(phr)	Tm (°C)	Tc (°C)
PP	166.6	113.1
PP-g-MA	160.9	127.9
PP/PS (75/25)	166.8	114.2
55/20/1/24/0	167.1	124
55/20/1/24/0.16	166.7	127.6
55/20/1/24/0.32	167.2	129.6
55/20/1/24/0.48	167.4	131.2
55/20/2/23/0	166.5	122.5
55/20/2/23/0.16	166.5	128
55/20/2/23/0.32	167.2	129.7
55/20/2/23/0.48	167	131.8
55/20/3/22/0	167.2	121.7
55/20/3/22/0.16	166.7	127.5
55/20/3/22/0.32	167	129.5
55/20/3/22/0.48	167.3	131.9

3/22/0.48 phr [Fig. 3(d)] shows a higher torque value, which can be attributed to the formation of various PP-*g*-MA-*co*-TGDDM-*co*-SMA copolymers in the blend, as well as the molecular weight increase of SMA and PP-*g*-MA, respectively.

Morphologies

One of the key objectives in reactive compatibilization is to control the domain size of the minor phase. Factors influencing the polymer blend morphology development include the viscosity ratio of the blend constituents, composition, processing conditions, elasticity ratio, and interfacial modification.[17] Generally, immiscible and incompatible blends possess high interfacial tension, which results in coarser morphology than corresponding adequately compatibilized blends. Figure 4(a) shows the SEM micrograph of the cryogenic-fracture surface of the PP/PS = 75/25 blend where the PS phase was etched out by the solvent. Large and irregular PS domains can be easily identified in this incompatibilized PP/PS blend. The interface is also quite sharp, indicating poor interfacial adhesion and high interfacial tension of PP and PS. The SEM micrographs of the PP/PS = 75/25 series blends with various amounts of PP-*g*-MA and SMA are shown in Figure 4(b–d). Compared to Figure 4(a), no obvious reduction in PS domain was observed, implying that without a coupler, PP-*g*-MA and SMA alone are unable to effectively compatibilize the incompatible PP/PS blend. A significant reduction of the PS domain sizes was found with the presence of TGDDM in these PP/PP-*g*-MA/SMA/PS blends, as shown in Figure 5(a–c). As mentioned above, an efficient compatibilizer functions as an emulsifier to reduce the interfacial tension of the immiscible blend, leading to finer domain sizes and broad interface thickness. During the melt-blending process, the multifunctional TGDDM can react simultaneously with PP-*g*-MA and SMA to form various *in situ* PP-*g*-MA-*co*-TGDDM-*co*-SMA copolymers at the interfaces and results in finer PS domains. Better compatibilization can be achieved by using higher TGDDM content, as the PS domains are finer in Figure 5(b,c). These morphological findings provide further evidence to explain the observed trend of the mechanical properties.

Thermal properties

Table IV summarizes the DSC results of the pure components, uncompatibilized and compatibilized blends. Here we present only the data of Tm and Tc to discuss the effect of compatibilizer on the crystalline phase behavior. The effect of compatibilizer on the amorphous phase is not explored because the Tg of PP and PP-*g*-MA is difficult to observe due to their high crystallinity, while SMA is a minor component whose Tg is not easily detected by DSC. Duvall et al.[16] demonstrated that PP-*g*-MA with low MA content is capable of cocrystallizing with PP and no phase separation between PP-*g*-MA crystal and PP crystal was observed by DSC and hot stage microscopy. The cocrystallization behavior between bulk PP and PP segment of PP-*g*-MA was also proven by WAXD analysis by Ma et al.[17] In Table IV the Tm values of the PP phase in the blends are almost the same as that of pure PP, regardless of the quantity of the TGDDM. This result suggests that in our blend systems PP-*g*-MA cocrystallizes with PP and is miscible in the crystal form. The Tc can be used as an indicator of the crystallization rate. In

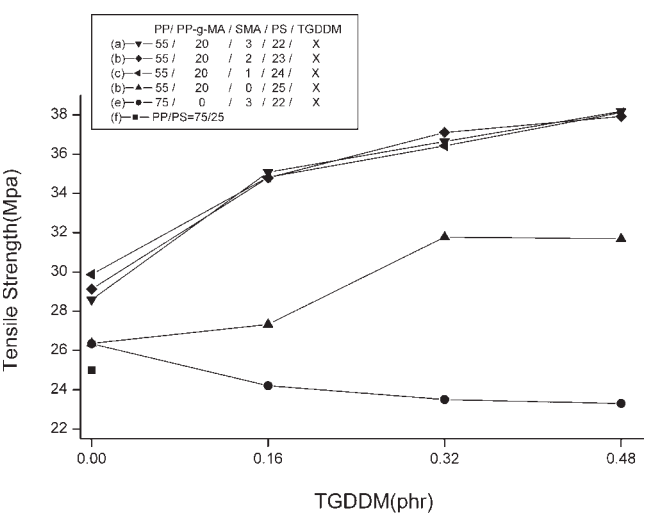

Figure 6 Effect of TGDDM amount on the tensile strength of various PP/PP-*g*-MA/SMA/PS blends.

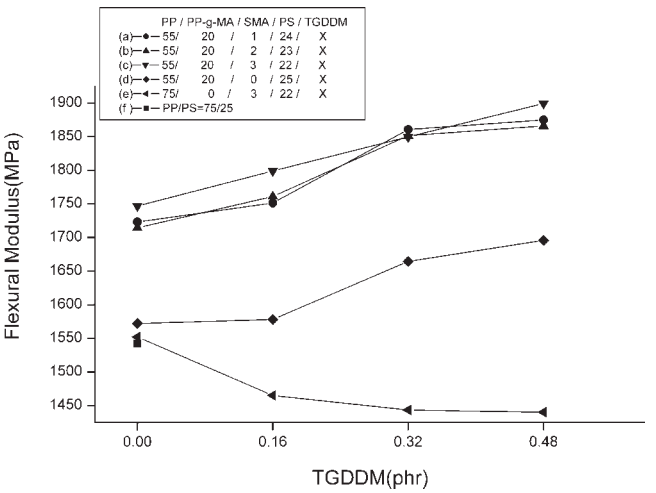

Figure 7 Effect of TGDDM amount on the flexural modulus of various PP/PP-*g*-MA/SMA/PS blends.

Table IV it is shown that for various blend compositions the Tc of the PP component in blends is increased with increasing TGDDM quantity. The highest Tc of the PP component in the compatibilized blend is ~19°C higher than pure PP (131.9°C vs. 113.1°C). The significant change in Tc can be attributed to the finer PS domains in the compatibilized blends observed in the morphology section, which function as effective nucleating agents and further enhance the crystallization rate of PP. From the polymer processing point of view, the Tc increase of the crystalline component in polymer blends is quite beneficial for injection molding because of the dramatic cycle time reduction. Higher Tc means the products in the mold solidify faster and can be ejected in a shorter time. As a result, the processing cycle time can be decreased and the overall productivity will be improved.

Mechanical properties

The resulting mechanical properties can serve as an indicator of the effectiveness of a compatibilizer in immiscible or incompatible blends. Generally, it is expected that the mechanical properties of the compatibilized polymer blends will be improved compared to the corresponding incompatibilized ones because of the lower interfacial tension and enhanced interfacial adhesion of the compatibilized blends, making stress transfer more efficient between phases during fracture. Figures 6 and 7 show the tensile strength at break and flexural modulus of various incompatibilized and compatibilized PP/PS blends. With the addition of the TGDDM coupler, both tensile strength and flexural modulus are improved for all physically functionalized PP/PS blends [Figs. 6(a–c), 7(a–c)]. The observed mechanical property improvements imply that those *in situ* formed PP-*g*-MA-*co*-TGDDM-*co*-SMA copolymers tend to anchor along the interface and broaden the interface region, resulting in finer domain and better stress transfer. Blends of which only the PP component was physical functionalized [Figs. 6(d), 7(d)] also exhibit better mechanical properties with the addition of TGDDM. The mechanical properties increase is mainly due to the molecular weight increase of PP-*g*-MA, as the PS phase was not physically functionalized and formation of the *in situ* copolymer is impossible. However, for the PP/PS/PP-*g*-MA/SMA = 75/22/0/3 series blends [Figs. 6(e), 7(e)], the presence of TGDDM is detrimental to tensile strength as well as flexural modulus. As discussed in the torque versus time section, the molecular weight increase of SMA is very significant with the addition of TGDDM compared to that of PP-*g*-MA. Without the presence of PP-*g*-MA in the blend, only the very high molecular weight, i.e., lightly crosslinked, SMA will be formed, which will possibly phase separate from the PS domain and result in poorer mechanical properties.

CONCLUSIONS

FTIR analysis provides direct evidence of reactions of TGDDM with PP-*g*-MA and SMA during melt blending. The torque versus time plot shows that the reactivity of TGDDM with SMA is significantly higher than that of TGDDM with PP-*g*-MA. The PS domain size is significantly reduced for those compatibilized PP/PS blends from the SEM graphs. The crystallization temperature of PP in the compatibilized blends increases with decreasing PS domain size, whereas the melting temperature remains close to that of pure PP. The tensile strength and flexural modulus of the compatibilized blends are substantially improved compared to noncompatibilized blends. Reactive compatibilization cannot be achieved unless PP and PS are both physically functionalized. A small quantity of the TGDDM is critical to function as a coupler in the PP/PS blend during melt-blending.

References

1. Utracki, L. A. Commercial Polymer Blends; Chapman & Hall: London, 1998
2. Paul, D. R.; Bucknall, C. B. Polymer Blends; Wiley: New York, 2000.
3. Barlow, J. W.; Paul, D. R. Polym Eng Sci 1984, 24, 525.
4. Lyatskaya, Y.; Balazs, A. C. Macromolecules, 1996, 29, 7581.
5. Baker, W. E.; Scott, C. E.; Hu, G. H. Reactive Polymer Blending; Hanser: Munich, 2001.
6. Ju, M. Y.; Chang, F. C. Polymer 2000, 41, 1719.

7. Chiou, K. C.; Chang, F. C. J Polym Sci B Polym Phys 2000, 38, 23.
8. Chu, M. Y.; Chen, M. Y.; Chang, F. C. Macromol Chem Phys 2000, 201, 2298.
9. Radonjic, G.; Musil V.; Smit, I. J Appl Polym Sci 1998, 69, 2625.
10. Hlavata, D.; Horak, Z.; Hromadkova, J. J Polym Sci B Polym Phys 1999, 37, 1647.
11. Raghu, P.; Nere, C. K.; Jagtap, R. N. J Appl Polym Sci 2003, 88, 266.
12. Xie, X. M.; Zheng, X. Mater Design 2001, 22, 11.
13. Kim, S. H.; Kim, J. K.; Park, C. E. Polymer 1997, 38, 1809.
14. Sun, Y.; Willemse, R.; Liu, T.; Baker, W. Polymer 1998, 39, 2201.
15. Gonzalez-Montiel, A.; Keskkula, H.; Paul, D. R. J Polym Sci B Polym Phys 1995, 33, 1751.
16. Duvall, I.; Sellitti, C.; Myers, C.; Hiltner, A.; Bear, E. J Appl Polym Sci 1994, 52, 207.
17. Ma, Z. L.; Gao, J. G.; Niu, H. J.; Ding, H. T.; Zhang, J. J Appl Polym Sci 2002, 85, 257.